

Nitrogen-doped carbon modified nickel catalyst for the hydrogenation of levulinic acid under mild conditions

Liang Jiang^{‡1}, Guangyue Xu^{‡1}, Yao Fu *¹

1. Anhui Province Key Laboratory of Biomass Clean Energy, CAS Key Laboratory of Urban Pollutant Conversion, University of Science and Technology of China, Hefei 230026. Institute of Energy, Hefei Comprehensive National Science Center, Hefei 230031.

E-mail for Y. Fu: fuyao@ustc.edu.cn

‡ These authors contributed equally to this work

Table S1. Comparison of reaction conditions of hydrogenation of levulinic acid over different nickel-based catalysts.

Entry	Catalyst	Ni content (wt. %)	Reaction conditions	Selectivity (%)	Ref.
1	Ni/MgO	44	150 °C, 1 MPa H ₂	93.3	1
2	Ni/Mg ₂ Al ₂ O ₅	40	160 °C, 3 MPa H ₂	99.7	2
3	Ni/ γ -Al ₂ O ₃	40	180 °C, 3 MPa H ₂	98.2	3
4	Ni/NCMs	6.3	200 °C, 3 MPa H ₂	99	4
5	Ni/Al ₂ O ₃	15	200 °C, 5 MPa H ₂	100	5
6	Ni/C-500	58.4	200 °C, 1 MPa H ₂	98.2	6
7	NiAl-LDH	7	200 °C, 3 MPa H ₂	100	7
8	Ni–MoOx/C	10	140 °C, 8 bar H ₂	97	8
9	Ni/Al ₂ O ₃ -CN-600	7.9	130 °C, 1 bar H ₂	> 99	This work

Table S2. Metal content of Ni/Al₂O₃-CN-T measured by ICP-OES.

Entry	Catalyst	Ni Content (wt %)
1	Ni/Al ₂ O ₃ -CN-500	7.1
2	Ni/Al ₂ O ₃ -CN-600	7.9
3	Ni/Al ₂ O ₃ -CN-700	8.3

Table S3. Surface atomic composition of Ni/Al₂O₃-CN-T measured by XPS.

Entry	Catalyst	Surface atomic composition (%)			
		Ni	Al	C	N
1	Ni/Al ₂ O ₃ -CN-500	1.29	25.0	26.1	0.7
2	Ni/Al ₂ O ₃ -CN-600	1.23	25.9	25.3	0.6
3	Ni/Al ₂ O ₃ -CN-700	0.93	27.3	23.9	0.4

Table S4. Textural and structural properties of NiO/Al₂O₃-CN-air and Ni/Al₂O₃-CN-T catalysts.

catalyst	Surface area (m ² /g)	Pore volume (cm ³ /g)	Pore diameter (nm)
NiO/Al ₂ O ₃ -CN-air	67.70	0.10	5.91
Ni/Al ₂ O ₃ -CN-500	240.29	0.18	4.54
Ni/Al ₂ O ₃ -CN-600	162.79	0.20	4.78
Ni/Al ₂ O ₃ -CN-700	145.12	0.20	5.49

Table S5. The effect of the reaction solvents on the hydrogenation of levulinic acid over different solvents.

Entry	Catalyst	Solvent	Conv.	Sele.	Ref.
1	Ru ₃ TPA	Methanol	92%	75%	
		Ethanol	91%	68%	
		Isopropanol	65%	61%	
		Butanol	52%	50%	9
		Dioxane	95%	100%	
		H ₂ O	80%	90%	
2	CuPS-R ₃₅₀ -C ₈ -R ₃₅₀	THF	95.7%	89.0%	
		Ethanol	81.6%	90.0%	10
		Water	45.5%	89.0%	
3	Ru-TS	THF	61%	0%	
		Methanol	95%	62%	
		Ethanol	98%	86%	11
		Butanol	80%	76%	
		Dioxane	21%	5%	
		H ₂ O	>99%	>99%	12

		Methanol	63%	32.8%	
		Ethanol	28%	>99%	
		Dioxane	0%	0%	
		THF	≈82%	-	
		H ₂ O	≈58%	-	
5	CuNi@SiO ₂	Isopropanol	99%	96.8%	13
		Dioxane	≈38%		
		Toluene	24%	87.5%	
		Dioxane	13%	30.8%	
6	Ni–MoO _x /C	H ₂ O	2%	100%	8
		No solvent	100%	97%	
		Water	67.5%	67.5%	
7	Ni _{4.59} Cu ₁ Mg _{1.58} Al _{1.96} Fe _{0.70}	Methanol	98.1%	98.1%	14
		H ₂ O	≈2%	≈99%	
		Methanol	≈ 80%	≈3%	
8	Ni/MgO	Ethanol	≈52%	≈30%	1
		isopropanol	100%	93.3%	
		Dioxane	≈89%	≈96%	
		THF	21%	95%	
		H ₂ O	>99%	>99%	
		Methanol	14%	0%	
9	Ni-Sn(1.4)/ AlOH	Ethanol	20%	0%	15
		Isopropanol	10%	0%	
		Dioxane	35%	97.1%	

		THF	14.7%	0%	
		H ₂ O	69.2%	99%	
10	Ru/N@CNTs	Methanol	40.4%	22%	16
		Ethanol	20%	35.5%	
		Isopropanol	12.1%	90%	
		Dioxane	21.9%	84.9%	
11	Ni/Al ₂ O ₃ -CN-600	THF	>99%	>99%	This work
		H ₂ O	96.2%	98.2%	
		Toluene	93.7%	97.3%	
		Methanol	>99%	86.6%	
		Ethanol	>99%	96.1%	
		Isopropanol	93.6%	98.2%	
		Dioxane	82.1%	96.6%	

Table S6. Ni contents of Ni/Al₂O₃ before and after recycle measured by ICP-OES.

Entry	Sample	Ni contents (wt %)
1	Fresh Ni/Al ₂ O ₃ -CN-600	7.9
2	Ni/Al ₂ O ₃ -CN-600 after 5 runs	7.7
3	Fresh Ni/Al ₂ O ₃	9.4
4	Ni/Al ₂ O ₃ after 5 runs	7.0

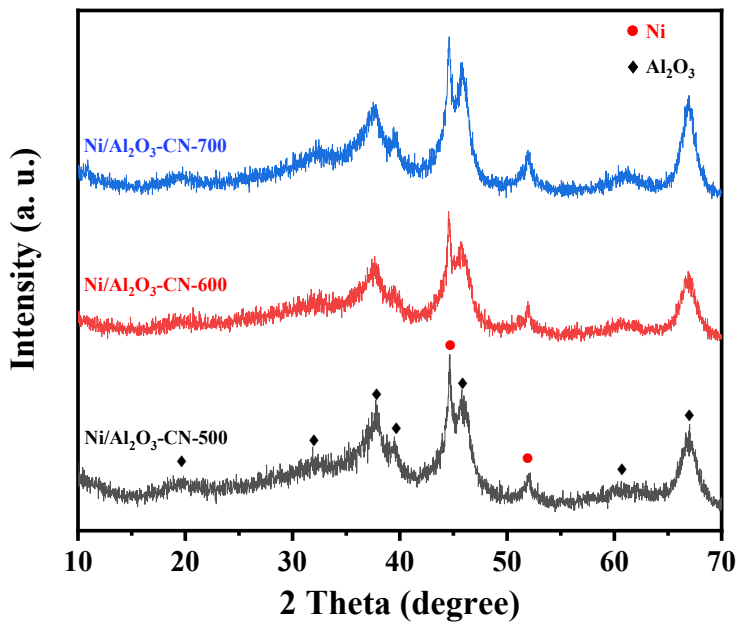


Figure S1. XRD pattern of the different Ni/Al₂O₃-CN-T catalysts.

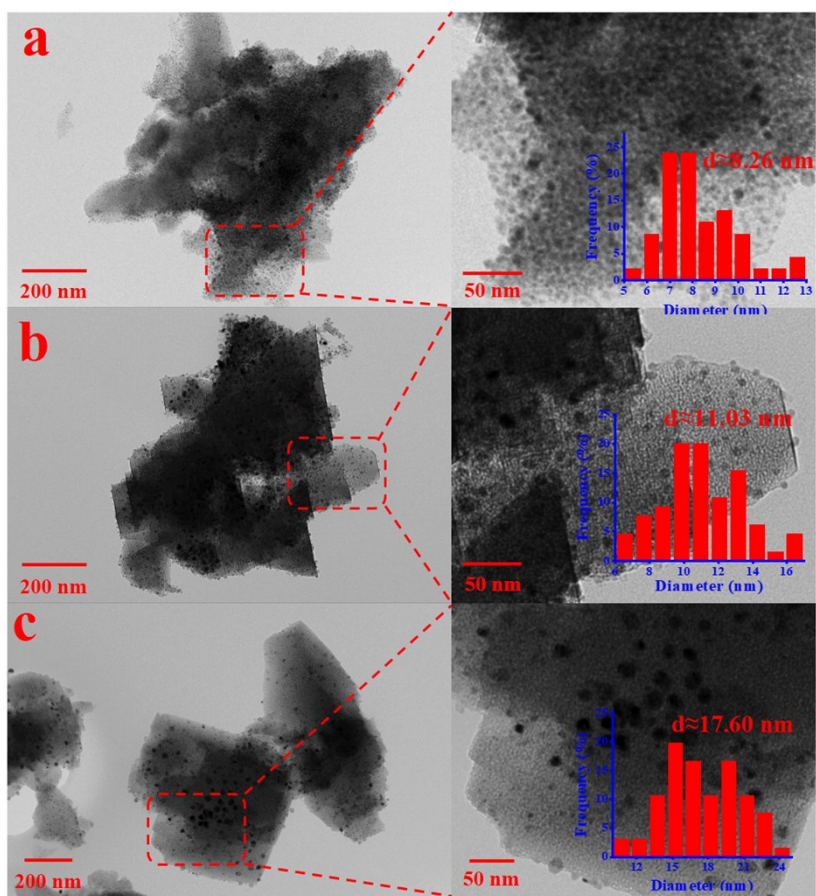


Figure S2. TEM images and average size distribution of nickel nanoparticles of the Ni/Al₂O₃-CN-500 (a), Ni/Al₂O₃-CN-600 (b) and Ni/Al₂O₃-CN-700 (c).

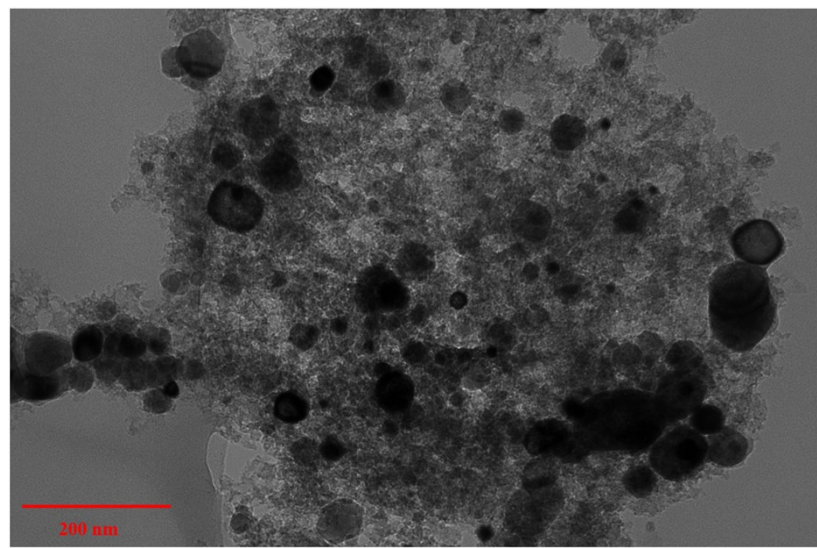


Figure S3. TEM image of Ni/CN-600.

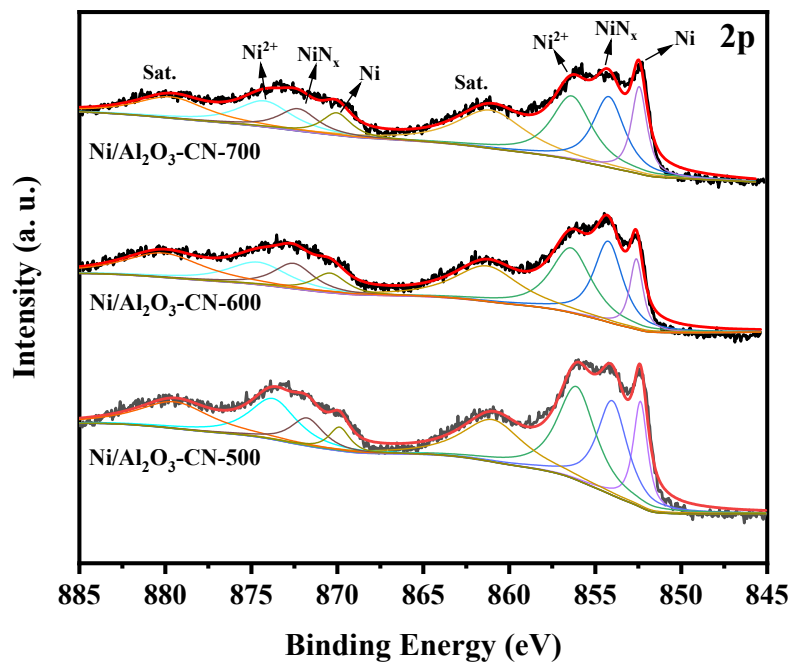


Figure S4. The Ni 2p XPS pattern of the different Ni/Al₂O₃-CN-T catalysts.

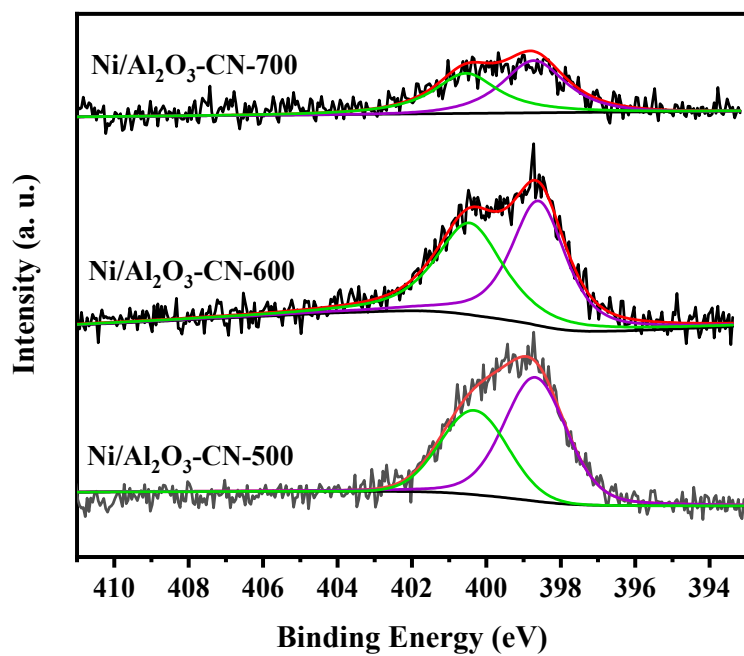


Figure S5. The N 1s XPS pattern of the different $\text{Ni}/\text{Al}_2\text{O}_3\text{-CN-T}$ catalysts.

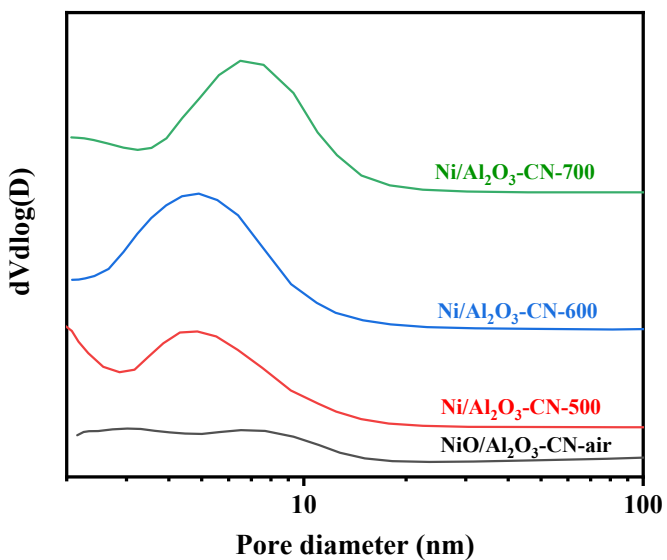
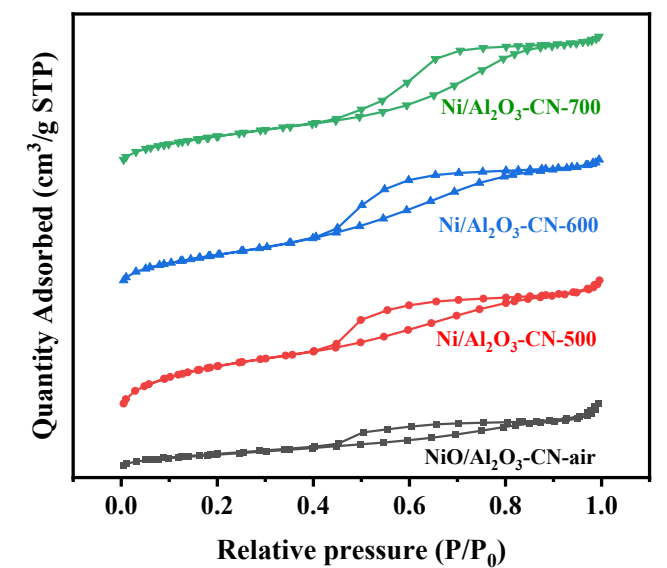


Figure S6. N₂ adsorption-desorption isotherms and pore size distributions of NiO/Al₂O₃-CN-air and the Ni/Al₂O₃-CN-T catalysts.

REFERENCES

1. Lv, J. K., Rong, Z. M., Wang, Y., Xiu, J. H., Wang, Y., Qu, J. P. Highly efficient conversion of biomass-derived levulinic acid into gamma-valerolactone over Ni/MgO catalyst. *RSC Adv.* **2015**, *5*, 72037-72045.
2. Jiang, K., Sheng, D., Zhang, Z. H., Fu, J., Hou, Z. Y., Liu, X. Y. Hydrogenation of levulinic acid to gamma-valerolactone in dioxane over mixed MgO-Al₂O₃ supported Ni catalyst. *Catal. Today*. **2016**, *274*, 55-59.
3. Fu, J., Sheng, D., Lu, X. Y. Hydrogenation of Levulinic Acid over Nickel Catalysts Supported on Aluminum Oxide to Prepare gamma-Valerolactone. *Catalysts*. **2016**, *6*, 6.
4. Liu, D. W., Zhang, L. N., Han, W. P., Tang, M. X., Zhou, L. G., Zhang, Y., Li, X. K., Qin, Z. F., Yang, H. Q. One-step fabrication of Ni-embedded hierarchically-porous carbon microspheres for levulinic acid hydrogenation. *Chem. Eng. J.* **2019**, *369*, 386-393.
5. Hengst, K., Schubert, M., Carvalho, H. W. P., Lu, C. B., Kleist, W., Grunwaldt, J. D. Synthesis of γ -valerolactone by hydrogenation of levulinic acid over supported nickel catalysts. *Appl. Catal., A*. **2015**, *502*, 18-26.
6. Xu, H., Hu, D., Yi, Z. X., Wu, Z. T., Zhang, M., Yan, K. Solvent Tuning the Selective Hydrogenation of Levulinic Acid into Biofuels over Ni-Metal Organic Framework-Derived Catalyst. *ACS Appl. Energy Mater.* **2019**, *2*, 6979-6983.
7. Gundekari, S., Srinivasan, K. In situ generated Ni(0)@boehmite from NiAl-LDH: An efficient catalyst for selective hydrogenation of biomass derived levulinic acid to gamma-valerolactone. *Catal. Commun.* **2017**, *102*, 40-43.

8. Shimizu, K., Kanno, S., Kon, K. Hydrogenation of levulinic acid to γ -valerolactone by Ni and MoO_x co-loaded carbon catalysts. *Green Chem.* **2014**, *16*, 3899-3903.
9. Koley, P., Rao, B. S., Shit, S. C., Sabri, Y., Mondal, J., Tardio, J., Lingaiah, N. One-pot conversion of levulinic acid into gamma-valerolactone over a stable Ru tungstophosphoric acid catalyst. *Fuel.* **2021**, *289*, 119900.
10. Tsou, Y. J., To, T. D., Chiang, Y. C., Lee, J. F., Kumar, R., Chung, P. W., Lin, Y. C. Hydrophobic Copper Catalysts Derived from Copper Phyllosilicates in the Hydrogenation of Levulinic Acid to γ -Valerolactone. *ACS Appl. Mater. Interfaces.* **2020**, *12*, 54851-54861.
11. Almeida, L. D., Rocha, A. L. A., Rodrigues, T. S., Robles-Azocar, P. A. Highly selective hydrogenation of levulinic acid catalyzed by Ru on TiO₂-SiO₂ hybrid support. *Catal. Today.* **2020**, *344*, 158-165.
12. Li, S. P., Wang, Y. Y., Yang, Y. D., Chen, B. F., Tai, J., Liu, HZ., Han, B. X. Conversion of levulinic acid to γ -valerolactone over ultra-thin TiO₂ nanosheets decorated with ultrasmall Ru nanoparticle catalysts under mild conditions. *Green Chem.* **2019**, *21*, 770-774.
13. Pendem, S., Mondal, I., Shrotri, A., Rao, B. S., Lingaiah, N. Mondal, J Unraveling the structural properties and reactivity trends of Cu–Ni bimetallic nanoalloy catalysts for biomass-derived levulinic acid hydrogenation. *Sustainable Energy Fuels.* **2018**, *2*, 1516-1529.
14. Zhang, J., Chen, J. Z., Guo, Y. Y., Chen, L. M. Effective Upgrade of Levulinic Acid into γ -Valerolactone over an Inexpensive and Magnetic Catalyst Derived from

Hydrotalcite Precursor. *ACS Sustainable Chem. Eng.* **2015**, *3*, 1708-1714.

15. Rodiansono., Astuti, M. D., Hara, T., Ichikuni, N., Shimazu, S. Efficient hydrogenation of levulinic acid in water using a supported Ni–Sn alloy on aluminium hydroxide catalysts. *Catal. Sci. Technol.* **2016**, *6*, 2955-2961.
16. Meng, Z., Liu, Y., Yang, G. X., Cao, Y. H., Wang, H. J., Peng, F., Liu, P. F., Yu, H. Electron-rich ruthenium on nitrogen-doped carbons promoting levulinic acid hydrogenation to γ -valerolactone: effect of metalsupport interaction. *ACS Sustainable Chem. Eng.* **2019**, *7*, 16501-16510.